



## Wentinoids A–F, six new isopimarane diterpenoids from *Aspergillus wentii* SD-310, a deep-sea sediment derived fungus†

Xin Li,<sup>‡,ab</sup> Xiao-Dong Li,<sup>‡,ab</sup> Xiao-Ming Li,<sup>a</sup> Gang-Ming Xu,<sup>a</sup> Yang Liu<sup>ab</sup> and Bin-Gui Wang<sup>\*a</sup>

Six new isopimarane-type diterpenoid derivatives, wentinoids A–F (**1–6**), along with a known congener (**7**), were identified from a culture of *Aspergillus wentii* SD-310, a fungus isolated from a deep-sea sediment sample. The structures of these compounds were determined by analysis of spectroscopic data, and their absolute configurations were established by single crystal X-ray analysis or TDDFT-ECD calculations. This is the first time to report the isolation of isopimarane analogues from the fungal species *Aspergillus wentii*. Among these compounds, wentinoid A (**1**) possesses a unique 20-acetal and a 7,20-oxa-bridged functionality, while wentinoid B (**2**) contains an unusual 8,20-lactone-bridged scaffold. Compound **1** exhibited potent inhibitory activities against four plant-pathogenic fungi.

Received 23rd November 2016  
Accepted 26th December 2016

DOI: 10.1039/c6ra27209f

[www.rsc.org/advances](http://www.rsc.org/advances)

## Introduction

Diterpenoids of the isopimarane-type comprise a structurally diverse and functionally noteworthy group of natural products, which are much more widely distributed in plants<sup>1–3</sup> than in fungi.<sup>4</sup> A number of isopimarane analogues have been proven to act as ecologically and biologically functional substances. Typical examples of isopimarane diterpenoids with ecological-related activities are pedinophyllols, which were isolated from the Chinese liverwort *Pedinophyllum interruptum* and exhibited germination inhibition for *Arabidopsis thaliana* seeds.<sup>5</sup> Some isopimarane derivatives displayed cytotoxicity,<sup>6,7</sup> anti-microbial,<sup>8,9</sup> anti-malarial,<sup>10</sup> anti-inflammatory,<sup>11</sup> and anti-virus<sup>12</sup> properties as well as inhibitory activities against acetylcholinesterase,<sup>13</sup>  $\alpha$ -glucosidase,<sup>3</sup> and nitric oxide production.<sup>2</sup> As part of our ongoing efforts to discover bioactive metabolites from marine-derived fungi,<sup>14–16</sup> we recently focused our attention on *Aspergillus wentii* SD-310, a fungal strain obtained from a deep-sea sediment sample. As a result, a series of 20-nor-isopimarane derivatives were isolated and identified.<sup>15,16</sup> Further work on this fungus has now resulted in the isolation of six new

isopimarane-type diterpenoid derivatives, wentinoids A–F (**1–6**), together with a known compound **7**. The planar structures of compounds **1–6** were established on the basis of spectroscopic analysis, and the absolute configurations were confirmed by single-crystal X-ray diffraction analysis or ECD calculations. These compounds represents the first example of isopimarane analogues isolated from the fungal species *A. wentii*, with wentinoid A (**1**) belongs to a rarely described class of tetracyclic isopimaranes, which contain an oxa-bridge-ring. In contrast to other related congeners, compound **1** possesses a unique 20-acetal moiety and 7,20-oxa-bridged functionality. Meanwhile, wentinoid B (**2**) represents a tetracyclic isopimarane and contains an unusual 8,20-lactone-bridged scaffold. The anti-microbial activities of the isolated compounds against 11 human-, and aqua-pathogenic bacteria and seven plant-pathogenic fungi were evaluated. Details of the isolation, structure elucidation, and biological activities of compounds **1–7** are described herein.

## Results and discussion

The mycelia and culture broth of *A. wentii* SD-310 were extracted with MeOH and EtOAc, respectively, to obtain two extracts, which were combined and purified by a combination of column chromatography (CC) on Si gel, Lobar LiChroprep RP-18, and Sephadex LH-20, to yield compounds **1–7** (Fig. 1).

Wentinoid A (**1**) was initially obtained as colorless oily powder. Its molecular formula was determined to be  $C_{21}H_{32}O_4$  by HRESIMS, indicating six degrees of unsaturation. The  $^1H$  and  $^{13}C$  NMR, DEPT, and HMQC spectroscopic data (Tables 1 and 2) revealed that **1** contained a tetra-substituted olefin ( $\delta_C$  131.4, C-8;  $\delta_C$  141.6, C-9), a vinyl group ( $\delta_C$  145.8,  $\delta_H$  6.03, dd,  $J$  = 17.7,

<sup>a</sup>Laboratory of Marine Biology and Biotechnology, Qingdao National Laboratory for Marine Science and Technology, Key Laboratory of Experimental Marine Biology, Institute of Oceanology, Chinese Academy of Sciences, Nanhai Road 7, Qingdao 266071, P. R. China. E-mail: wangbg@ms.qdio.ac.cn

<sup>b</sup>University of Chinese Academy of Sciences, Yuquan Road 19A, Beijing 100049, P. R. China

† Electronic supplementary information (ESI) available: NMR and HRESIMS spectra of compounds **1–6**. CCDC 1462858, 1462859 and 1462860 for compounds **1**, **3**, and **5** respectively. For ESI and crystallographic data in CIF or other electronic format see DOI: 10.1039/c6ra27209f

‡ X. L. and X. D. L. contributed equally to this work.



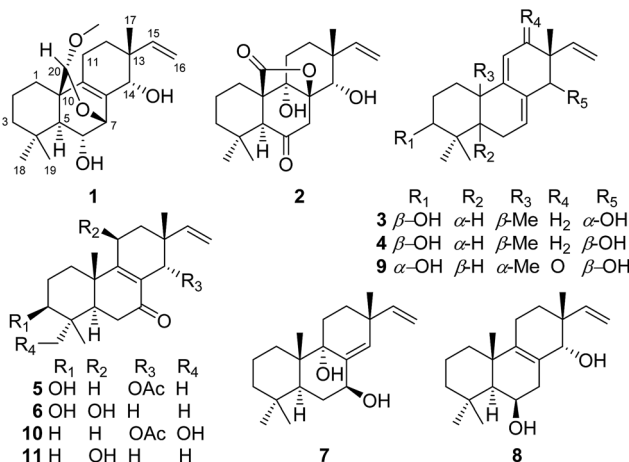


Fig. 1 Chemical structures of compounds 1–7 and reference compounds 8–11.

10.2 Hz, CH-15;  $\delta_C$  111.4,  $\delta_H$  4.98, d,  $J$  = 17.7 Hz, 4.96, d,  $J$  = 10.2 Hz, CH<sub>2</sub>-16), an acetal carbon ( $\delta_C$  97.7, C-20), three oxygenated methines ( $\delta_{C/H}$  68.0/3.68, C-6;  $\delta_{C/H}$  72.7/4.14, C-7;  $\delta_{C/H}$  71.1/3.49, C-14), and a methoxy group ( $\delta_{C/H}$  54.2/3.13, C-21). The protons of methoxy group (H<sub>3</sub>-21) showed HMBC correlation to C-20, which implied a connection between the methoxy and

C-20 (Fig. 2). The attachment of the *gem*-dimethyl groups (C-18 and C-19) to the quaternary carbon C-4 were identified by their mutual HMBC correlations, along with correlations from H<sub>3</sub>-18 and H<sub>3</sub>-19 to C-3, C-4, and C-5. Furthermore, signals for three quaternary carbons, an  $sp^3$  methine, five aliphatic methylenes, and a singlet methyl were also observed from the NMR spectra.

Comparison of the NMR data of **1** with that of kaempulchraol C (**8**),<sup>1</sup> an isopimarane-type diterpenoid isolated from rhizomes of *Kaempferia pulchra*, revealed that the structures of these two compounds are very similar. However, signals for the bridgehead methyl (C-20) and the methylene group (C-7) in **8** were absent in the NMR spectra of **1**. Instead, resonances for an acetal carbon (C-20) and an oxygenated methine group (C-7) were observed in the NMR spectra of **1**. In addition, C-7 and C-20 connected each other *via* an oxygen atom, and this deduction was verified by the key HMBC correlations from H-7 to C-5, C-9, and C-20 and from H-20 to C-1, C-5, C-7, and C-9. The planar structure of **1** was fully defined by the HMBC data as shown in Fig. 2.

The relative configuration of **1** was assigned by analysis of the NOESY data (Fig. 3). While NOE correlations from H-5 to H-3 $\alpha$ , 6-OH, H-7, H-11 $\alpha$ , and H<sub>3</sub>-18 and from H-15 to H-11 $\alpha$  and H-12 $\alpha$  indicated the cofacial orientation of these groups, correlations from H-6 to H<sub>3</sub>-19 and H-20, from H-11 $\beta$  to H<sub>3</sub>-17, and

Table 1  $^1H$  NMR data for compounds 1–6 (500 MHz,  $J$  in Hz, measured in DMSO- $d_6$ )

Position	1	2	3	4	5	6
1	$\alpha$ 1.49 m $\beta$ 1.86 m	$\alpha$ 1.35 td (13.6, 3.6) $\beta$ 1.78 d (13.6)	$\alpha$ 1.34 td (12.9, 5.4) $\beta$ 1.78 dt (12.9, 5.4)	$\alpha$ 1.34 td (12.8, 5.4) $\beta$ 1.79 dt (12.8, 3.3)	$\alpha$ 1.44 m $\beta$ 1.78 m	$\alpha$ 1.35 td (13.1, 3.6) $\beta$ 2.45 m
2	1.45 m	$\alpha$ 1.46 m $\beta$ 1.89 dtt (13.6, 13.6, 3.6)	1.54 m	1.55 m	1.60 m	$\alpha$ 1.55 m $\beta$ 1.61 m
3	$\alpha$ 1.17 m $\beta$ 1.41 m	$\alpha$ 1.08 td (13.6, 3.6) $\beta$ 1.30 d (13.6)	2.99 m	2.99 m	3.11 m	3.05 m
5	0.75 d (3.5)	2.84 s	1.08 dd (11.6, 4.5)	1.05 dd (11.7, 4.5)	1.62 dd (14.3, 4.2)	1.48 m
6	3.68 m	—	$\alpha$ 2.13 m $\beta$ 2.05 m	$\alpha$ 2.05 m $\beta$ 2.00 m	$\alpha$ 2.34 dd (18.2, 4.2) $\beta$ 2.43 dd (18.2, 14.3)	$\alpha$ 2.27 dd (18.6, 3.3) $\beta$ 2.48 dd (18.6, 3.5)
7	4.14 d (4.2)	$\alpha$ 3.35 d (16.4) $\beta$ 2.28 d (16.4)	5.77 brs	5.70 brs	—	—
11	$\alpha$ 2.17 d (17.7) $\beta$ 1.75 ddd (17.7, 11.6, 5.4)	$\alpha$ 1.69 dt (14.8, 3.6) $\beta$ 1.50 dd (14.8, 3.6)	5.26 brs	5.28 brs	$\alpha$ 2.49 m $\beta$ 2.27 m	4.38 brs
12	$\alpha$ 1.67 td (11.6, 5.4) $\beta$ 1.29 m	$\alpha$ 2.08 td (13.6, 3.6) $\beta$ 1.18 d (13.6)	$\alpha$ 2.20 dd (17.8, 4.3) $\beta$ 1.97 dd (17.8, 4.3)	$\alpha$ 1.93 dd (18.0, 4.6) $\beta$ 2.12 m	$\alpha$ 1.75 m $\beta$ 1.48 m	$\alpha$ 1.80 dd (12.0, 6.0) $\beta$ 1.46 dd (12.0, 6.0)
14	3.49 s	3.22 s	3.71 s	3.54 s	5.58 s	$\alpha$ 2.10 d (17.2) $\beta$ 1.97 d (17.2)
15	6.03 dd (17.7, 10.2)	5.98 dd (17.5, 11.1)	5.85 dd (16.9, 10.1)	5.73 dd (17.6, 10.9)	5.79 dd (17.2, 11.2)	5.69 dd (17.5, 10.8)
16	4.98 d (17.7) 4.96 d (10.2)	4.93 d (17.5) 4.92 d (11.1)	4.93 dd (16.9, 1.6) 4.90 dd (10.1, 1.6)	4.95 d (17.6) 4.87 d (10.9)	4.97 dd (17.2) 4.96 d (11.2)	4.88 d (10.8) 4.80 d (17.5)
17	0.87 s	0.94 s	0.95 s	0.91 s	0.78 s	0.99 s
18	0.94 s	1.12 s	0.88 s	0.88 s	0.89 s	0.87 s
19	0.92 s	0.95 s	0.78 s	0.78 s	0.79 s	0.78 s
20	4.80 s	—	0.88 s	0.88 s	1.07 s	1.25 s
21	3.13 s	—	—	—	—	—
22	—	—	—	—	1.83 s	—
3-OH	—	—	4.41 s	4.42 s	4.52 d (4.3)	4.47 brs
6-OH	4.61 brs	—	—	—	—	—
11-OH	—	—	—	—	—	4.92 d (6.0)
14-OH	3.95 brs	—	4.61 s	4.56 s	—	—



Table 2  $^{13}\text{C}$  NMR data for compounds 1–6 (125 MHz, measured in  $\text{DMSO}-d_6$ )

Position	1	2	3	4	5	6
1	25.9 $\text{CH}_2$	24.1 $\text{CH}_2$	34.4 $\text{CH}_2$	35.0 $\text{CH}_2$	33.6 $\text{CH}_2$	34.6 $\text{CH}_2$
2	17.7 $\text{CH}_2$	16.9 $\text{CH}_2$	26.8 $\text{CH}_2$	27.4 $\text{CH}_2$	27.0 $\text{CH}_2$	27.0 $\text{CH}_2$
3	40.7 $\text{CH}_2$	41.9 $\text{CH}_2$	76.3 $\text{CH}$	76.8 $\text{CH}$	75.6 $\text{CH}$	76.1 $\text{CH}$
4	32.9 $\text{qC}$	32.4 $\text{qC}$	38.0 $\text{qC}$	38.5 $\text{qC}$	38.4 $\text{qC}$	38.5 $\text{qC}$
5	54.7 $\text{CH}$	56.3 $\text{CH}$	47.5 $\text{CH}$	48.0 $\text{CH}$	47.5 $\text{CH}$	49.8 $\text{CH}$
6	68.0 $\text{CH}$	207.4 $\text{qC}$	22.5 $\text{CH}_2$	23.0 $\text{CH}_2$	34.7 $\text{CH}_2$	32.7 $\text{CH}_2$
7	72.7 $\text{CH}$	48.1 $\text{CH}_2$	121.0 $\text{CH}$	123.8 $\text{CH}$	196.7 $\text{qC}$	199.9 $\text{qC}$
8	131.4 $\text{qC}$	85.4 $\text{qC}$	134.0 $\text{qC}$	134.7 $\text{qC}$	127.4 $\text{qC}$	128.9 $\text{qC}$
9	141.6 $\text{qC}$	74.5 $\text{qC}$	144.6 $\text{qC}$	144.4 $\text{qC}$	170.0 $\text{qC}$	163.3 $\text{qC}$
10	44.0 $\text{qC}$	53.8 $\text{qC}$	35.5 $\text{qC}$	36.0 $\text{qC}$	39.0 $\text{qC}$	39.4 $\text{qC}$
11	21.3 $\text{CH}_2$	26.0 $\text{CH}_2$	113.5 $\text{CH}$	114.6 $\text{CH}$	21.4 $\text{CH}_2$	65.3 $\text{CH}$
12	28.1 $\text{CH}_2$	24.3 $\text{CH}_2$	35.7 $\text{CH}_2$	34.2 $\text{CH}_2$	25.4 $\text{CH}_2$	44.0 $\text{CH}_2$
13	39.1 $\text{qC}$	39.8 $\text{qC}$	40.1 $\text{qC}$	40.3 $\text{qC}$	38.1 $\text{qC}$	34.8 $\text{qC}$
14	71.1 $\text{CH}$	72.5 $\text{CH}$	74.7 $\text{CH}$	75.1 $\text{CH}$	67.8 $\text{CH}$	34.0 $\text{CH}_2$
15	145.8 $\text{CH}$	147.7 $\text{CH}$	142.4 $\text{CH}$	145.2 $\text{CH}$	144.0 $\text{CH}$	145.5 $\text{CH}$
16	111.4 $\text{CH}_2$	110.4 $\text{CH}_2$	111.7 $\text{CH}_2$	111.6 $\text{CH}_2$	112.4 $\text{CH}_2$	111.2 $\text{CH}_2$
17	20.4 $\text{CH}_3$	21.5 $\text{CH}_3$	23.2 $\text{CH}_3$	21.0 $\text{CH}_3$	20.9 $\text{CH}_3$	27.6 $\text{CH}_3$
18	33.3 $\text{CH}_3$	32.4 $\text{CH}_3$	27.4 $\text{CH}_3$	27.9 $\text{CH}_3$	27.2 $\text{CH}_3$	27.6 $\text{CH}_3$
19	22.4 $\text{CH}_3$	19.1 $\text{CH}_3$	15.2 $\text{CH}_3$	15.7 $\text{CH}_3$	15.3 $\text{CH}_3$	15.5 $\text{CH}_3$
20	97.7 $\text{CH}$	176.7 $\text{qC}$	20.6 $\text{CH}_3$	21.0 $\text{CH}_3$	18.5 $\text{CH}_3$	18.5 $\text{CH}_3$
21	54.2 $\text{CH}_3$	—	—	—	168.8 $\text{qC}$	—
22	—	—	—	—	20.9 $\text{CH}_3$	—

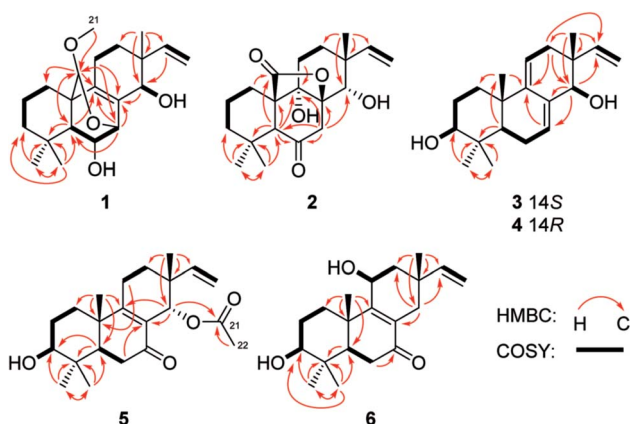


Fig. 2 Key COSY and HMBC correlations of compounds 1–6.

from H-12 $\beta$  to H-14 placed these groups on the opposite face. To confirm the structure as well as the relative and absolute configurations, crystallization of **1** was performed. After many attempts, single crystals suitable for X-ray analysis were obtained by slow evaporation of a solution of **1** in MeOH. Once the X-ray crystallographic experiment was conducted, the structure and absolute configuration of **1** were confidently assigned as depicted (Fig. 4).

Wentinoid B (**2**) was obtained as colorless oil. The molecular formula  $\text{C}_{20}\text{H}_{28}\text{O}_5$ , implying seven degrees of unsaturation, was established by HRESIMS. The  $^1\text{H}$  NMR spectrum displayed typical signals for a vinyl group (H-15 and H-16), three singlet methyls ( $\text{H}_3\text{-}17\text{-H}_3\text{-}19$ ), a pair of methylene protons (H-7), an oxygenated methine (H-14), an aliphatic methine (H-5), and other ten aliphatic protons (Table 1). Its  $^{13}\text{C}$  NMR data (Table 2) exhibited the presence of 20 carbon

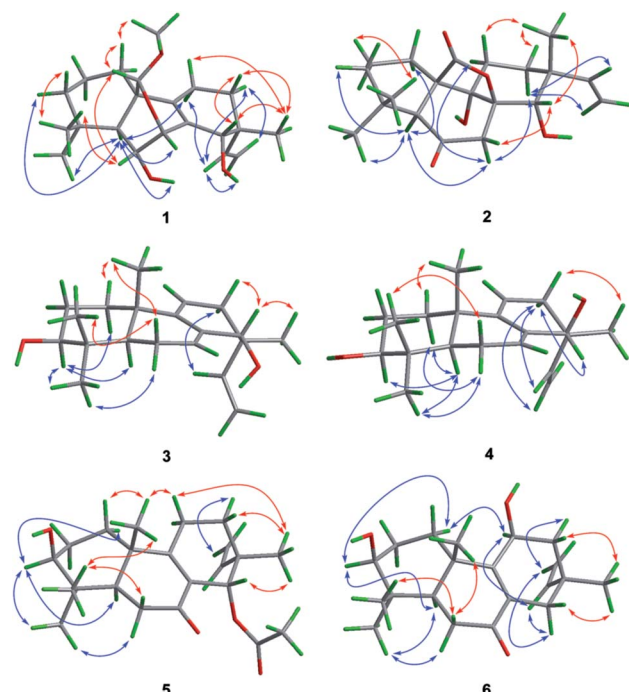


Fig. 3 Key NOESY correlations of 1–6.

signals, which were sorted by DEPT and HSQC spectrum into three methyls, seven methylenes (one olefinic), three methines (one oxygenated and one olefinic), and seven quaternary (one lactone, one ketone and one oxygenated aliphatic quaternary) carbons. Interpretation of the COSY and HSQC spectra of **2** resulted in the elucidation of two discrete proton spin-coupling systems corresponding to a  $-\text{CH}_2\text{-CH}_2\text{-CH}_2-$  unit (C-1 through C-3) and a  $-\text{CH}_2\text{-CH}_2-$  unit (C-11 and C-12). Key



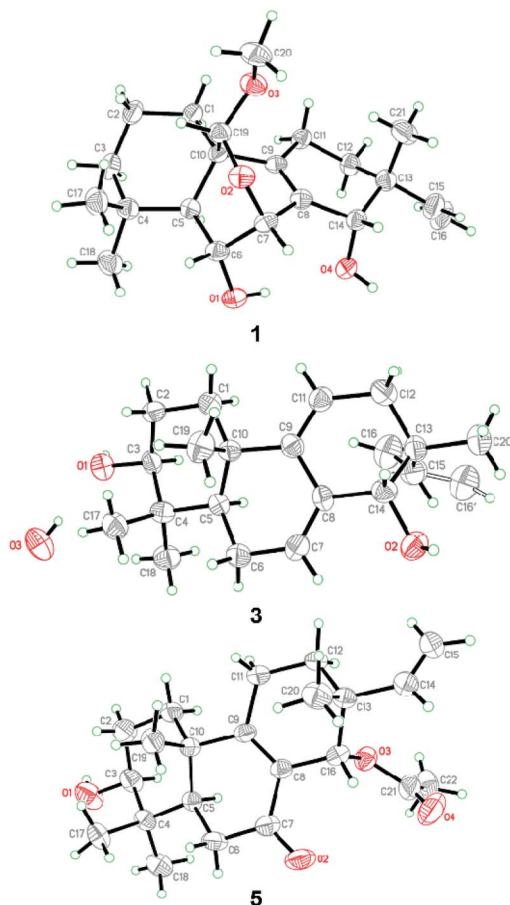


Fig. 4 X-ray crystallographic structures of compounds 1, 3, and 5 (note: different numbering systems are used for the structures in the text).

HMBC correlations shown in Fig. 2 suggested the presence of an isopimarane-type diterpenoid skeleton for 2. The ketone and two hydroxy groups were placed at C-6, C-9 and C-14, respectively, as supported by HMBC correlations from H-5 and H<sub>2</sub>-7 to C-6 and C-9 and from H<sub>2</sub>-7 and H<sub>3</sub>-17 to C-14. The remaining oxygen atom and one degree of unsaturation, together with the consideration of the strongly deshielded nature of C-8 ( $\delta_C$  85.4) suggesting the presence of a lactone bridge between C-8 and C-10 *via* C-20. Thus, the entire structure of compound 2 was identified as shown in Fig. 1.

The relative configuration of 2 was determined by NOESY experiment and by comparison of 1D NMR data of 2 with related analogues. Key NOE correlations from H-5 to H-7 $\alpha$  and H<sub>3</sub>-18, from H-7 $\alpha$  to H-11 $\alpha$  and H-12 $\alpha$  and from H-12 $\alpha$  to H-15 placed these protons on the same face of the molecule. Moreover, NOE correlations from H-7 $\beta$  to H-14 and from H<sub>3</sub>-17 to H-11 $\beta$  suggested these groups on the opposite face of the molecule. The assignment of the  $\beta$ -orientation of the lactone group was established by analysis of the magnetic anisotropic effect as the method reported by the previous ref. 7. The deshielding effect from the carbonyl at C-20 resulted in downfielded chemical shift of H-2 $\beta$ . The chemical shift of C-9 ( $\delta_C$  74.5) in <sup>13</sup>C-NMR was consistent with those of related

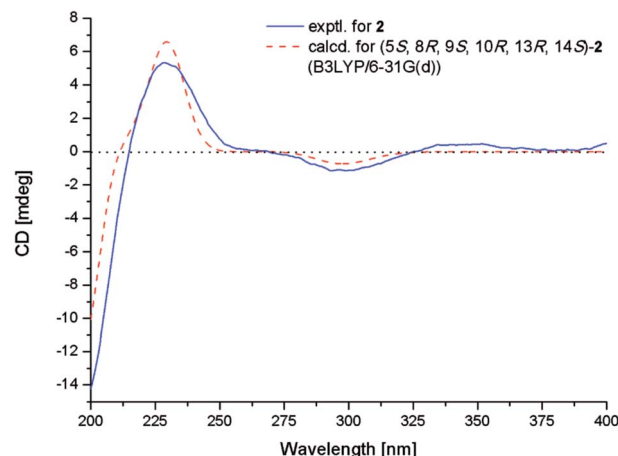


Fig. 5 Experimental and calculated ECD spectra of 2.

diterpenoids with an  $\alpha$ -OH at C-9 ( $\delta_C$  73.6–75.6).<sup>7</sup> In order to determine the absolute configuration of 2, conformational analysis and TDDFT-ECD calculations were performed on the arbitrarily chosen of (5S,8R,9S,10R,13R,14S)-2. The DFT reoptimization of the initial MM + conformers of the selected enantiomer at the B3LYP/6-31G(d) level in gas phase afforded minimum energy conformers. The TDDFT-ECD spectra of the conformers were calculated with B3LYP and the 6-31G(d) basis set. The computed ECD spectra of (5S,8R,9S,10R,13R,14S)-2 matched well to the experimental ECD spectrum, which showed positive cotton effects (CEs) near 228 and 344 nm and negative CE near 299 nm (Fig. 5).

Wentinoid C (3) was originally obtained as colorless oily powder. The HREIMS data of 3 determined the molecular formula C<sub>20</sub>H<sub>30</sub>O<sub>2</sub>. The <sup>1</sup>H and <sup>13</sup>C NMR data (Tables 1 and 2) are very similar to those of *ent*-3 $\beta$ ,14 $\alpha$ -hydroxypimar-7,9(11),15-triene-12-one (9),<sup>17</sup> implying the same carbon skeleton for both compounds. However, resonance at  $\delta_C$  202.2 for the ketone group at C-12 in 9 was not observed in that of 3. Instead, signals for a methylene group at  $\delta_C$  35.7 were found in the <sup>13</sup>C-NMR spectra of 3. Compared to 9, obvious upfielded shift for C-11, C-13, and C-15, and downfielded shift for C-17 in the <sup>13</sup>C NMR spectrum of 3 were also observed. These data indicated the replacement of a ketone group in 9 by a methylene group in 3, which was consistent with the molecular formula. The COSY correlations from H<sub>2</sub>-11 to H<sub>2</sub>-12 as well as key HMBC correlations from H<sub>2</sub>-12 to C-9, C-14, and C-15 and from H<sub>3</sub>-17 to C-12 verified the above deduction (Fig. 2).

NOE correlations from H-1 $\beta$  to H<sub>3</sub>-20, from H-6 $\beta$  to H<sub>3</sub>-19 and H<sub>3</sub>-20, and from H-14 to H-12 $\beta$ , H<sub>3</sub>-17 and H<sub>3</sub>-20 revealed that these protons are on the same side, while correlations from H-3 to H-1 $\alpha$ , H-5, and H<sub>3</sub>-18 and from H-6 $\alpha$  to H<sub>3</sub>-18 indicated that they are on the other side. To unequivocally determine the absolute configuration, single crystals were cultivated upon slow evaporation of the solvent (MeOH) and a Cu/K $\alpha$  X-ray diffraction analysis was conducted. The final refinement of the X-ray data resulted in a 0.0(14) Flack parameter, allowing for the unambiguous assignment of the absolute configuration as shown in Fig. 4.



Wentinoid D (**4**) was obtained as colorless oil. The molecular formula was determined as  $C_{20}H_{30}O_2$ , same as that of **3**, on the basis of HREIMS data. The similar UV absorptions to those of compound **3** implied that **4** was an analogue of **3**. The NMR spectra of **4** were also close to that of **3**. Inspection of the  $^1H$  and  $^{13}C$  NMR data (Tables 1 and 2) suggested that **4** is a diastereomer of **3**, epimeric at C-14. This was supported by the minor differences on the chemical shifts for C-7, C-12, C-15, and C-17 in **4**, which were from  $\gamma$ -gauche effect caused by the inversion of the absolute configuration at C-14. NOE correlations from  $H_{12\beta}$  to  $H_{3-17}$  and from  $H_{12\alpha}$  to  $H_{14}$ ,  $H_{15}$ , and  $H_{2-16}$  confirmed this deduction (Fig. 3). The structure of **4** was thus assigned as shown in Fig. 1.

Wentinoid E (**5**), initially obtained as colorless oily powder, had the molecular formula  $C_{22}H_{32}O_4$  (seven degrees of unsaturation) as determined by HRESIMS data. Detailed comparison of the NMR data of **5** with those of sorgerolone (**10**)<sup>13</sup> revealed that compound **5** had the same basic structure as **10**. However, signals for the methylene group resonating at  $\delta_C$  34.4 and  $\delta_H$  1.35/1.56 ( $CH_2$ -3) and those of the hydroxymethyl group at  $\delta_C$  70.6 and  $\delta_H$  3.15/3.43 ( $CH_2$ -18) in **10** disappeared in the NMR spectra of **5**. Instead, signals for an oxygenated methine group at  $\delta_C$  75.6 and  $\delta_H$  3.11 ( $CH$ -3) and a methyl at  $\delta_C$  27.2 and  $\delta_H$  0.89 ( $CH_3$ -18) were observed (Tables 1 and 2). The above observation suggested that compound **5** was 3-hydroxy-18-dehydroxy derivative of **10**. The cross-peaks from  $H_{2-2}$  to  $H_{2-1}$  and  $H_{3-3}$  and from  $H_{3-3}$  to 3-OH in the COSY spectrum as well as the correlations from  $H_{5-5}$  to C-3, from  $H_{3-18}$  and  $H_{3-19}$  to C-3, C-4, and C-5 in the HMBC spectrum confirmed the above deduction (Fig. 2).

The relative configuration of **5** was deduced from NOESY data. NOE correlations from  $H_{1\beta}$  to  $H_{3-20}$ , from  $H_{11\beta}$  to  $H_{3-17}$  and  $H_{3-20}$ , and from  $H_{3-17}$  to  $H_{14}$  placed these protons on the same face of the molecule, while  $H_{3-3}$ ,  $H_{5-5}$ , and  $H_{3-18}$  had  $\alpha$ -orientation as confirmed by the correlations from  $H_{3-3}$  to  $H_{1\alpha}$ ,  $H_{5-5}$ , and  $H_{3-18}$  (Fig. 3). An X-ray crystallographic experiment confirmed the absolute configuration of **5** as depicted (Fig. 4). The Cu/K $\alpha$  radiation used for the X-ray diffraction allowed the assignment of the absolute configuration of all of the stereogenic centers in **5** as  $3S$ ,  $5R$ ,  $10S$ ,  $13R$  and  $14S$ .

Wentinoid F (**6**), was obtained as colorless oil, was assigned the molecular formula  $C_{20}H_{30}O_3$  on the basis of HRESIMS data. The  $^{13}C$  NMR spectrum of **6** exhibited signals similar to those presented in 11 $\beta$ -hydroxy-7-oxopimar-8(9),15-dien (**11**)<sup>18</sup> except for the methylene group at  $\delta_C$  35.9 (C-3) in  $^{13}C$  NMR spectrum of **11** was replaced by an oxymethine unit at  $\delta_C$  76.1 (C-3) in that of **6**, indicating that **6** was C-3 hydroxylated derivative of **11**. The 2D NMR correlations supported this inference by the COSY correlations from  $H_{2-2}$  to  $H_{2-1}$  and  $H_{3-3}$  and HMBC correlations from  $H_{3-18}$  and  $H_{3-19}$  to C-3.

The NOE correlations from  $H_{1\alpha}$  to  $H_{3-3}$  and  $H_{11}$ , from  $H_{3-3}$  to  $H_{3-18}$ , from  $H_{6\alpha}$  to  $H_{3-18}$ , from  $H_{11}$  to  $H_{15}$ , and from  $H_{14\alpha}$  to  $H_{15}$  indicated the same orientation of these groups (Fig. 3), whereas correlations from  $H_{6\beta}$  to  $H_{3-20}$  revealed that these groups were on the other face. The absolute configuration of **6** was established by TDDFT-ECD calculations. The experimental ECD spectrum of **6** matched well with that calculated for  $(3S,5R,10S,11S,13R)-6$  (Fig. 6). The structure and

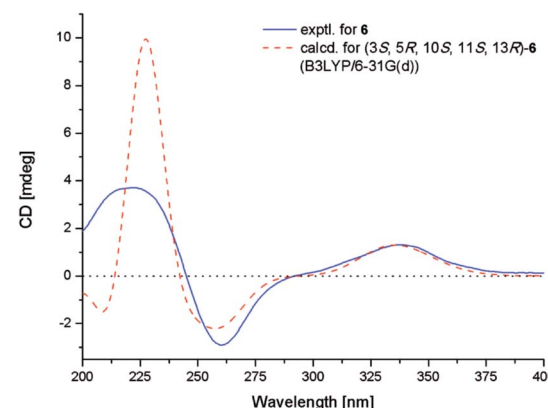
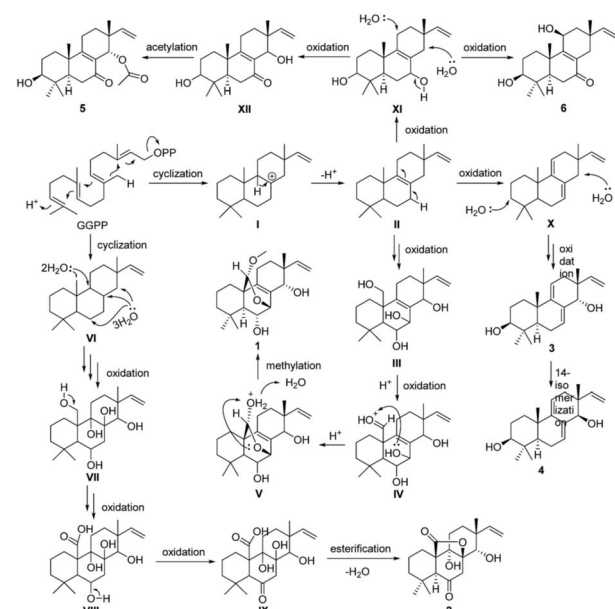


Fig. 6 Experimental and calculated ECD spectra of **6**.

absolute configuration of **6** were thus assigned as shown in Fig. 1.

A plausible biosynthetic pathway for compounds **1–6** is proposed as shown in Scheme 1. In this pathway, compounds **1–6** are produced from geranylgeranylpyrophosphate (GGPP). Intermediate **II**, produced by reduction of **I**, is presumed to be a common biosynthetic precursor of compounds **1** and **3–6**. After oxidation of **II** at C-7, C-14, and C-20, C-20 of intermediate **III** is further oxidized giving aldehyde derivative **IV**. Aldolization between the aldehyde group at C-20 and 7-OH in **IV** gives **V**, and successive methylation of 20-OH yields compound **1**. Deprotonation of H-7 and H-11 in **II** leads to **X**, which is further oxidized to give isomers **3** and **4**. Meanwhile, oxidation of C-3 and C-7 in **II** gives **XI**. Further oxidation of C-11 in **XI** yields **6**, whereas oxidation of C-14 in **XI** gives **5** via **XII**. After cyclization, GGPP is converted to **IX** via intermediates **VI–IX** by multistep oxidation of C-8, C-9, C-14, and C-20. Following esterification between carboxyl at C-20 and 8-OH, compound **2** is formed.



Scheme 1 Proposed biosynthetic pathway for compounds **1–6**.



The isolated compounds were tested against 11 human-, and aqua-pathogenic bacteria and seven plant-pathogenic fungi. Compound **1** exhibited selective activities against *Phytophthora parasitica*, *Fusarium oxysporum* f. sp. *lycopersici*, *Fusarium graminearum*, and *Botryosphaeria dothidea* with MIC values of 8.0, 4.0, 1.0, and 4.0  $\mu\text{g mL}^{-1}$ , respectively, which were comparable to that of the positive control, amphotericin B (MIC = 2.0, 1.0, 1.0, and 2.0  $\mu\text{g mL}^{-1}$ , respectively). However, other compounds didn't displayed potent inhibitory activity.

## Conclusions

In summary, we isolated and characterized six new compounds wentinoids A–F (**1**–**6**), which are new members of highly oxygenated isopimarane-type diterpenoids. Among them, wentinoid A (**1**) contains unusual 20-acetal moiety and 7,20-oxa-bridged functionality, whereas wentinoid B (**2**) possesses a novel 8,20-lactone-bridged scaffold. A plausible biosynthesis mechanism for compounds **1**–**6** was proposed. The discovery of these compounds might provide further insight into the biosynthesis of isopimarane family and also provide new targets for synthetic or biosynthetic studies. Compound **1**, which may prove useful as antifungal agent, exhibited potent antimicrobial activities against some plant pathogenic fungi.

## Experimental section

### General experimental procedures

Melting points were determined with an SGW X-4 micromelting-point apparatus. Optical rotations were measured on an Optical Activity AA-55 polarimeter. UV spectra were measured on a PuXi TU-1810 UV-visible spectrophotometer. CD spectra were acquired on a JASCO J-715 spectropolarimeter. 1D and 2D NMR spectra were recorded at 500 and 125 MHz for  $^1\text{H}$  and  $^{13}\text{C}$ , respectively, on a Bruker Avance 500 MHz spectrometer with TMS as internal standard. Mass spectra were obtained on a VG Autospec 3000 or an API QSTAR Pulsar 1 mass spectrometer. Analytical and semi-preparative HPLC were performed using a Dionex HPLC system equipped with a P680 pump, an ASI-100 automated sample injector, and a UVD340U multiple wavelength detector controlled by Chromeleon software (version 6.80). Commercially available Si gel (200–300 mesh, Qingdao Haiyang Chemical Co.), Lobar LiChroprep RP-18 (40–63  $\mu\text{m}$ , Merck), and Sephadex LH-20 (Pharmacia) were used for open column chromatography. All solvents were distilled prior to use.

### Fungal material

The isolation and identification of the fungal material were identical to those described in our previous report.<sup>15</sup> The strain is preserved at the Key Laboratory of Experimental Marine Biology, Institute of Oceanology of the Chinese Academy of Sciences (IOCAS), with accession number SD-310.

### Cultivation

For chemical investigations, the fungal strain was dynamic fermented at a 500 L fermentator preloaded with 300 L of

sterilized liquid medium containing 50% (v/v) sea water (20% potato, 2% glucose, 0.5% peptone, and 0.3% yeast extract, pH 6.0) for 7 days at room temperature.

### Extraction and isolation

The whole fermented cultures were filtered to separate the broth from the mycelia. The former was extracted three times with EtOAc, while the latter was extracted three times with a mixture of acetone and water (80 : 20, v/v). The acetone solution was evaporated under reduced pressure to afford an aqueous solution, which was then extracted three times with EtOAc. Since the TLC and HPLC profiles of the two EtOAc solutions from the broth and mycelia were almost identical, they were combined and concentrated under reduced pressure to give an extract (34.7 g) for further separation.

The combined extract was fractionated by silica gel vacuum liquid chromatography (VLC) using a stepwise gradient of a mixture of petroleum ether (PE)-ethyl acetate (EtOAc) (1 : 0, 50 : 1, 20 : 1, 5 : 1, 2 : 1 and 1 : 1) and  $\text{CH}_2\text{Cl}_2$ -MeOH (20 : 1, 10 : 1, 5 : 1 and 0 : 1) to yield 10 major primary fractions (Fr.1–Fr.10). Fr.4 (7.1 g) was separated by CC on Lobar LiChroprep C<sub>18</sub> eluting with MeOH-H<sub>2</sub>O gradient to give nine subfractions (Fr. 4.1–4.9). Further purification of Fr. 4.4 by CC on silica gel with a  $\text{CH}_2\text{Cl}_2$ -MeOH gradient (from 50 : 1 to 5 : 1) yielded Frs. 4.4.1–4.4.9, and then Fr. 4.4.3 was purified by CC on silica gel eluted with PE-EtOAc 5 : 1 to afford compounds **3** (10.9 mg) and **4** (8.3 mg). Fr. 4.5 was also resolved (Fr. 4.5.1–4.5.9) by CC on silica gel eluting with a  $\text{CH}_2\text{Cl}_2$ -MeOH gradient (from 50 : 1 to 5 : 1). Fr. 4.5.5 was further subjected to CC on silica gel eluting with a PE-EtOAc gradient (from 5 : 1 to 2 : 1) to yield compounds **1** (14.4 mg) and **2** (8.7 mg). Fr. 4.6 was chromatographed over silica gel ( $\text{CH}_2\text{Cl}_2$ -MeOH 50 : 1–15 : 1) to get Fr. 4.6.8, which was then purified by preparative TLC (PE-EtOAc 5 : 1) to give compound **5** ( $R_f$  = 0.4, 5.8 mg) and **6** ( $R_f$  = 0.6, 3.5 mg). Fr. 4.2 was subfractioned by CC on silica gel eluting with PE-EtOAc 15 : 1, then further purified by Sephadex LH-20 (MeOH) to yield **7** (6.6 mg).

**Wentinoid A (1).** Colorless oily powder.  $[\alpha]_{25}^D$  −114 ( $c$  0.22, MeOH). mp 125–127 °C. UV (MeOH)  $\lambda_{\text{max}}$  (log  $\epsilon$ ): 204 (2.07), 229 (1.63) nm. ECD (MeCN,  $\lambda$  [nm] ( $\Delta\epsilon$ ),  $c$  =  $1.1 \times 10^{-3}$  M): 207 (−16.0).  $^1\text{H}$  and  $^{13}\text{C}$ -NMR: see Tables 1 and 2 ESIMS (positive):  $m/z$  371 [M + Na]<sup>+</sup>. HRESIMS (positive):  $m/z$  371.2203 ([M + Na]<sup>+</sup>, calcd for  $\text{C}_{21}\text{H}_{32}\text{O}_4\text{Na}$  371.2193).

**Wentinoid B (2).** Colorless oil.  $[\alpha]_{25}^D$  −21 ( $c$  0.48, MeOH). UV (MeOH)  $\lambda_{\text{max}}$  (log  $\epsilon$ ): 209 (2.99), 270 (2.30) nm. ECD (MeCN,  $\lambda$  [nm] ( $\Delta\epsilon$ ),  $c$  =  $1.1 \times 10^{-3}$  M): 228 (+2.9), 301 (−0.6), 348 (+0.2) nm.  $^1\text{H}$  and  $^{13}\text{C}$ -NMR: see Tables 1 and 2 ESIMS (positive):  $m/z$  371 [M + Na]<sup>+</sup>. HRESIMS (positive):  $m/z$  371.1832 ([M + Na]<sup>+</sup>, calcd for  $\text{C}_{20}\text{H}_{28}\text{O}_5\text{Na}$  371.1829).

**Wentinoid C (3).** Colorless oily powder.  $[\alpha]_{25}^D$  −63 ( $c$  0.65, MeOH). mp 133–135 °C. UV (MeOH)  $\lambda_{\text{max}}$  (log  $\epsilon$ ): 238 (3.20) nm. ECD (MeCN,  $\lambda$  [nm] ( $\Delta\epsilon$ ),  $c$  =  $1.2 \times 10^{-3}$  M): 234 (−24.6).  $^1\text{H}$  and  $^{13}\text{C}$ -NMR: see Tables 1 and 2 EIMS:  $m/z$  302 [M]<sup>+</sup>, 287 [M − CH<sub>3</sub>]<sup>+</sup>, 284 [M − H<sub>2</sub>O]<sup>+</sup>, 270 [M − CH<sub>2</sub>O]<sup>+</sup>, 266 [M − 2H<sub>2</sub>O]<sup>+</sup>. HREIMS:  $m/z$  302.2248 ([M]<sup>+</sup>, calcd for  $\text{C}_{20}\text{H}_{30}\text{O}_2$  302.2246).

**Wentinoid D (4).** Colorless oil.  $[\alpha]_{25}^D -11$  (*c* 0.46, MeOH). UV (MeOH)  $\lambda_{\max}$  (log  $\varepsilon$ ): 240 (3.16) nm. ECD (MeCN,  $\lambda$  [nm] ( $\Delta\varepsilon$ ), *c* =  $1.2 \times 10^{-3}$  M): 238 (-24.6).  $^1\text{H}$  and  $^{13}\text{C}$ -NMR: see Tables 1 and 2 EIMS (negative): *m/z* 302 [M]<sup>+</sup>, 287 [M - CH<sub>3</sub>]<sup>+</sup>, 284 [M - H<sub>2</sub>O]<sup>+</sup>, 270 [M - CH<sub>2</sub>O]<sup>+</sup>, 266 [M - 2H<sub>2</sub>O]<sup>+</sup>. HREIMS (positive): *m/z* 302.2242 ([M]<sup>+</sup>, calcd for C<sub>20</sub>H<sub>30</sub>O<sub>2</sub> 302.2246).

**Wentinoid E (5).** Colorless oily powder.  $[\alpha]_{25}^D -30$  (*c* 0.46, MeOH). mp 137–139 °C. UV (MeOH)  $\lambda_{\max}$  (log  $\varepsilon$ ): 242 (3.31) nm. ECD (MeCN,  $\lambda$  [nm] ( $\Delta\varepsilon$ ), *c* =  $1.0 \times 10^{-3}$  M): 212 (-23.2), 242 (-57.2), 332 (+6.0) nm.  $^1\text{H}$  and  $^{13}\text{C}$ -NMR: see Tables 1 and 2 ESIMS (positive): *m/z* 361 [M + H]<sup>+</sup>. HRESIMS (positive): *m/z* 361.2367 ([M + H]<sup>+</sup>, calcd. for C<sub>22</sub>H<sub>33</sub>O<sub>4</sub> 361.2373).

**Wentinoid F (6).** Colorless oil.  $[\alpha]_{25}^D +82$  (*c* 0.17, MeOH). UV (MeOH)  $\lambda_{\max}$  (log  $\varepsilon$ ): 250 (2.05) nm. ECD (MeCN,  $\lambda$  [nm] ( $\Delta\varepsilon$ ), *c* =  $1.2 \times 10^{-3}$  M): 219 (+1.9), 261 (-1.6), 340 (+0.7) nm.  $^1\text{H}$  and  $^{13}\text{C}$ -NMR: see Tables 1 and 2 ESIMS (positive): *m/z* 341 [M + Na]<sup>+</sup>. HRESIMS (positive): *m/z* 341.2082 ([M + Na]<sup>+</sup>, calcd. for C<sub>20</sub>H<sub>30</sub>O<sub>3</sub>Na 341.2087).

### Computational section

Conformational searches were performed *via* the molecular mechanics using MM + method in HyperChem 8.0 software, and the geometries were further optimized at B3LYP/6-31G(d) level *in vacuo* *via* Gaussian 09 software to give the energy-minimized conformers. Then, the optimized conformers were subjected to the calculations of ECD spectra using TD-DFT at B3LYP/6-31G(d) level; solvent effects of the MeCN solution were evaluated at the same DFT level using the SCRF/PCM method.<sup>19</sup>

### X-ray crystallographic analysis of compounds 1, 3 and 5

All crystallographic data were collected on a Bruker Smart-1000 CCD diffractometer using graphite-monochromated Cu-K $\alpha$  radiation ( $\lambda = 1.54178$  Å) at 293(2) K. The data were corrected for absorption using the program SADABS.<sup>20</sup> The structures were solved by direct methods using the SHELXTL software package.<sup>21</sup> All non-hydrogen atoms were refined anisotropically. The H atoms were located by geometrical calculations, and their positions and thermal parameters were fixed during the structure refinement. The structures were refined using full-matrix least-squares techniques.<sup>22</sup>

**Crystal data for compound 1.** C<sub>21</sub>H<sub>32</sub>O<sub>4</sub>; F.W. = 348.47; orthorhombic space group P2<sub>1</sub>2<sub>1</sub>2<sub>1</sub>; unit cell dimensions *a* = 8.8580(6) Å, *b* = 12.4336(7) Å, *c* = 17.5420(12) Å, *V* = 1932.0(2) Å<sup>3</sup>,  $\alpha = \beta = \gamma = 90^\circ$ ; *Z* = 4; *d*<sub>calcd</sub> = 1.198 mg m<sup>-3</sup>; crystal dimensions 0.40 × 0.37 × 0.30 mm;  $\mu$  = 0.647 mm<sup>-1</sup>; and *F*(000) = 760. The 2860 measurements yielded 1907 independent reflections after equivalent data were averaged and Lorentz and polarization corrections were applied. The final refinement provided *R*<sub>1</sub> = 0.0894 and *wR*<sub>2</sub> = 0.1289 [*I* > 2 $\sigma$ (*I*)]. The Flack parameter was 0.0(5) in the final refinement for all 2860 reflections, with 1907 Friedel pairs.

**Crystal data for compound 3.** C<sub>20</sub>H<sub>30</sub>O<sub>2</sub>·H<sub>2</sub>O; F.W. = 320.46; orthorhombic space group P2<sub>1</sub>2<sub>1</sub>2<sub>1</sub>; unit cell dimensions *a* = 6.6729(5) Å, *b* = 11.9119(9) Å, *c* = 23.5741(18) Å, *V* = 1873.8(2) Å<sup>3</sup>,  $\alpha = \beta = \gamma = 90^\circ$ ; *Z* = 4; *d*<sub>calcd</sub> = 1.136 mg m<sup>-3</sup>; crystal dimensions 0.23 × 0.18 × 0.07 mm;  $\mu$  = 0.583 mm<sup>-1</sup>; and

*F*(000) = 704. The 3169 measurements yielded 1091 independent reflections after equivalent data were averaged and Lorentz and polarization corrections were applied. The final refinement provided *R*<sub>1</sub> = 0.2224 and *wR*<sub>2</sub> = 0.2979 [*I* > 2 $\sigma$ (*I*)]. The Flack parameter was 0.0(14) in the final refinement for all 3169 reflections, with 1091 Friedel pairs.

**Crystal data for compound 5.** C<sub>22</sub>H<sub>32</sub>O<sub>4</sub>; F.W. = 360.48; orthorhombic space group P2<sub>1</sub>2<sub>1</sub>2<sub>1</sub>; unit cell dimensions *a* = 9.4327(6) Å, *b* = 13.1356(9) Å, *c* = 16.7370(9) Å, *V* = 2073.8(2) Å<sup>3</sup>,  $\alpha = \beta = \gamma = 90^\circ$ ; *Z* = 4; *d*<sub>calcd</sub> = 1.155 mg m<sup>-3</sup>; crystal dimensions 0.45 × 0.25 × 0.20 mm;  $\mu$  = 0.620 mm<sup>-1</sup>; and *F*(000) = 784. The 2922 measurements yielded 2104 independent reflections after equivalent data were averaged and Lorentz and polarization corrections were applied. The final refinement provided *R*<sub>1</sub> = 0.0722 and *wR*<sub>2</sub> = 1211 [*I* > 2 $\sigma$ (*I*)]. The Flack parameter was 0.0(4) in the final refinement for all 2922 reflections, with 2104 Friedel pairs.

### Antimicrobial assay

Antimicrobial assay against eleven human-, and aqua-pathogenic bacteria *P. aeruginosa*, *E. tarda*, *A. hydrophilia*, *M. luteus*, *E. tarda*, *E. coli*, *V. parahaemolyticus*, *S. aureus*, *V. alginolyticus*, *V. harveyi*, and *E. tarda* as well as seven plant pathogenic fungi *C. albicans*, *P. parasitica*, *C. nicotianae*, *A. alternate*, *F. oxysporum* f. sp. *lycopersici*, *F. Graminearum*, and *B. dothidea* was carried out using the well diffusion method.<sup>23</sup> Chloramphenicol and Amphotericin B were used as a positive control for the bacteria and fungi, respectively.

### Acknowledgements

Financial support from the Ministry of Science and Technology of China (2012AA092104) and from the Scientific and Technological Innovation Project of Qingdao National Laboratory for Marine Science and Technology (No. 2015ASKJ02) is gratefully acknowledged. B.-G. Wang acknowledges the Taishan Scholar Project from Shandong Province and X.-D. Li thanks the China Postdoctoral Science Foundation Grant (2016LH00033) for the support to the work.

### Notes and references

- 1 N. N. Win, T. Ito, S. Aimaiti, H. Imagawa, H. Ngwe, I. Abe and H. Morita, *J. Nat. Prod.*, 2015, **78**, 1113.
- 2 K. Jiang, L. L. Chen, S. F. Wang, Y. Wang, Y. Li and K. Gao, *J. Nat. Prod.*, 2015, **78**, 1037.
- 3 N. N. Win, T. Ito, T. Matsui, S. Aimaiti, T. Kodama, H. Ngwe, Y. Okamoto, M. Tanaka, Y. Asakawa, I. Abe and H. Morita, *Bioorg. Med. Chem. Lett.*, 2016, **26**, 1789.
- 4 X. K. Xia, J. Qi, Y. Y. Liu, A. R. Jia, Y. G. Zhang, C. H. Liu, C. L. Gao and Z. G. She, *Mar. Drugs*, 2015, **13**, 1124.
- 5 N. Liu, R. J. Li, X. N. Wang, R. X. Zhu, L. Wang, Z. M. Lin, Y. Zhao and H. X. Lou, *J. Nat. Prod.*, 2013, **76**, 1647.
- 6 R. Wang, W. H. Chen and Y. P. Shi, *J. Nat. Prod.*, 2010, **73**, 17.



7 X. N. Wang, B. P. Bashyal, E. M. K. Wijeratne, J. M. U'Ren, M. X. Liu, M. K. Gunatilaka, A. E. Arnold and A. A. L. Gunatilaka, *J. Nat. Prod.*, 2011, **74**, 2052.

8 S. Dettrakul, P. Kittakoop, M. Isaka, S. Nopichai, C. Suyarnsestakorn, M. Tanticharoen and Y. Thebtaranonth, *Bioorg. Med. Chem. Lett.*, 2003, **13**, 1253.

9 D. Pattamadilok and R. Suttisri, *J. Nat. Prod.*, 2008, **71**, 292.

10 S. Thongnest, C. Mahidol, S. Sutthivaiyakit and S. Ruchirawat, *J. Nat. Prod.*, 2005, **68**, 1632.

11 Z. Y. Wu, Y. B. Zhang, K. K. Zhu, C. Luo, J. X. Zhang, C. R. Cheng, R. H. Feng, W. Z. Yang, F. Zeng, Y. Wang, P. P. Xu, J. L. Guo, X. Liu, S. H. Guan and D. A. Guo, *J. Nat. Prod.*, 2014, **77**, 2342.

12 G. J. Zhang, Y. H. Li, J. D. Jiang, S. S. Yu, X. J. Wang, P. Y. Zhuang, Y. Zhang, J. Qu, S. G. Ma, Y. Li, Y. B. Liu and D. Q. Yu, *Tetrahedron*, 2014, **70**, 4494.

13 A. Yılmaza, P. Çağlarc, T. Dirmencid, N. Görenc and G. Topçu, *Nat. Prod. Commun.*, 2012, **7**, 693.

14 P. Zhang, L. H. Meng, A. Mándi, T. Kurtán, X. M. Li, Y. Liu, X. Li, C. S. Li and B. G. Wang, *Eur. J. Org. Chem.*, 2014, 4029.

15 X. D. Li, X. M. Li, X. Li, G. M. Xu, Y. Liu and B. G. Wang, *J. Nat. Prod.*, 2016, **79**, 1347.

16 X. Li, X. M. Li, X. D. Li, G. M. Xu, Y. Liu and B. G. Wang, *RSC Adv.*, 2016, **6**, 75981.

17 R. W. Denton, W. W. Harding, C. I. Anderson, H. Jacobs, S. McLean and W. F. Reynolds, *J. Nat. Prod.*, 2001, **64**, 829.

18 A. C. Pinto and C. Borges, *Phytochemistry*, 1983, **22**, 2011.

19 M. J. Frisch, G. W. Trucks, H. B. Schlegel, G. E. Scuseria, M. A. Robb, J. R. Cheeseman, G. Scalmani, V. Barone, B. Mennucci, G. A. Petersson, H. Nakatsuji, M. Caricato, X. Li, H. P. Hratchian, A. F. Izmaylov, J. Bloino, G. Zheng, J. L. Sonnenberg, M. Hada, M. Ehara, K. Toyota, R. Fukuda, J. Hasegawa, M. Ishida, T. Nakajima, Y. Honda, O. Kitao, H. Nakai, T. Vreven, J. A. Montgomery Jr, J. E. Peralta, F. Ogliaro, M. Bearpark, J. J. Heyd, E. Brothers, K. N. Kudin, V. N. Staroverov, T. Keith, R. Kobayashi, J. Normand, K. Raghavachari, A. Rendell, J. C. Burant, S. S. Iyengar, J. Tomasi, M. Cossi, N. Rega, J. M. Millam, M. Klene, J. E. Knox, J. B. Cross, V. Bakken, C. Adamo, J. Jaramillo, R. Gomperts, R. E. Stratmann, O. Yazyev, A. J. Austin, R. Cammi, C. Pomelli, J. W. Ochterski, R. L. Martin, K. Morokuma, V. G. Zakrzewski, G. A. Voth, P. Salvador, J. J. Dannenberg, S. Dapprich, A. D. Daniels, O. Farkas, J. B. Foresman, J. V. Ortiz, J. Cioslowski and D. J. Fox, *Gaussian 09, revision D.01*, Gaussian, Inc., Wallingford, CT, 2013.

20 G. M. Sheldrick, *SADABS, Software for Empirical Absorption Correction*, University of Göttingen, Germany, 1996.

21 G. M. Sheldrick, *SHELXTL, Structure Determination Software Programs*, Bruker Analytical X-ray System Inc., Madison, WI, 1997.

22 G. M. Sheldrick, *SHELXL-97 and SHELXS-97, Program for X-ray Crystal Structure Solution and Refinement*, University of Göttingen, Germany, 1997.

23 S. K. S. Al-Burtamani, M. O. Fatope, R. G. Marwah, A. K. Onifade and S. H. Al-Saidi, *J. Ethnopharmacol.*, 2005, **96**, 107.

